Neuron 45, 553–564, February 17, 2005 ©2005 Elsevier Inc. DOI 10.1016/j.neuron.2005.01.036

Neuromodulation of Na^+ Channel Slow Inactivation via cAMP-Dependent Protein Kinase and Protein Kinase C

Yuan Chen,[1] Frank H. Yu,[1] D. James Surmeier,[2] Todd Scheuer,[1] and William A. Catterall[1,*]
[1] Department of Pharmacology
University of Washington
Seattle, Washington 98195
[2] Department of Physiology
Feinberg School of Medicine
Northwestern University
Chicago, Illinois 60611

Summary

Neurotransmitters modulate sodium channel availability through activation of G protein-coupled receptors, cAMP-dependent protein kinase (PKA), and protein kinase C (PKC). Voltage-dependent slow inactivation also controls sodium channel availability, synaptic integration, and neuronal firing. Here we show by analysis of sodium channel mutants that neuromodulation via PKA and PKC enhances intrinsic slow inactivation of sodium channels, making them unavailable for activation. Mutations in the S6 segment in domain III (N1466A,D) either enhance or block slow inactivation, implicating S6 segments in the molecular pathway for slow inactivation. Modulation of N1466A channels by PKC or PKA is increased, whereas modulation of N1466D is nearly completely blocked. These results demonstrate that neuromodulation by PKA and PKC is caused by their enhancement of intrinsic slow inactivation gating. Modulation of slow inactivation by neurotransmitters acting through G protein-coupled receptors, PKA, and PKC is a flexible mechanism of cellular plasticity controlling the firing behavior of central neurons.

Introduction

Voltage-gated sodium channels play a key role in neural signaling by initiating and propagating the action potential. Recent research also has highlighted the essential role of sodium channels in defining autonomous and synaptically driven activity (Colbert et al., 1997; Jung et al., 1997; Mickus et al., 1999; Johnston et al., 1999; Stuart, 1999; Stuart and Haussner, 2001; Gonzalez-Burgos and Barrioneuvo, 2001; Do and Bean, 2003; Maurice et al., 2004). Even small changes in sodium channel availability can alter action potential firing patterns, and point mutations in sodium channel α subunits underlie inherited forms of several human diseases, including epilepsy (Balser, 2002; Cannon, 1996; Maurice et al., 2004; Meisler et al., 2001).

Slow inactivation is an important factor that governs sodium channel availability. It differs from fast inactivation in both timescale (seconds rather than milliseconds) and in molecular mechanism (Rudy, 1978). Impairment of fast inactivation by site-directed mutations does not prevent slow inactivation and can increase it (Featherstone et al., 1996; Vedantham and Cannon, 1998). High-frequency spiking and prolonged depolarization drive sodium channels into the slow inactivated state. Exit from slow inactivation is very slow, requiring seconds. Slow inactivation increases the action potential threshold, limits the duration of bursts of action potentials, limits propagation of action potentials into dendritic regions, and is implicated in adaptation of pacemaking neurons to varying inputs (Colbert et al., 1997; Jung et al., 1997; Mickus et al., 1999; Carr et al., 2002; Do and Bean, 2003). Mutations that impair slow inactivation cause periodic paralysis of skeletal muscle and arrhythmias in heart (Ruff and Cannon, 2000; Wang et al., 2000), and many point mutations in different regions of sodium channels have small but significant effects on slow inactivation (Balser et al., 1996; Cummins and Sigworth, 1996; Kontis and Goldin, 1997; Mitrovic et al., 2000; Nau et al., 1999; O'Reilly et al., 2001; Ong et al., 2000; Todt et al., 1999; Vilin et al., 1999, 2001; Wang and Wang, 1997; Xiong et al., 2003). However, in spite of this extensive research, the molecular mechanism of slow inactivation is unknown, and no point mutations have been described that substantially block slow inactivation and thereby define its essential molecular determinants.

Neurotransmitters act through G protein-coupled receptors, protein kinase C (PKC), and protein kinase A (PKA), which phosphorylate brain sodium channels in vitro and in intact cells (Costa et al., 1982; Costa and Catterall, 1984a, 1984b; Rossie and Catterall, 1987, 1989; Rossie et al., 1988) and reduce peak sodium currents in both expression systems (Dascal and Lotan, 1991; Numann et al., 1991; Sigel and Baur, 1988) and neurons (Numann et al., 1991; Li et al., 1992; Surmeier et al., 1992; Cantrell et al., 1996, 1997, 1999a; Carr et al., 2002). Key sites of phosphorylation are located in the inactivation gate in the intracellular loop between domains III and IV (West et al., 1991) and in the large intracellular loop between domains I and II (Murphy et al., 1993; Smith and Goldin, 1996, 1997; Cantrell et al., 1997, 2002). Effective regulation by PKA requires interaction with A Kinase Anchoring Protein 15 (AKAP15), which also binds to the intracellular loop between domains I and II (Cantrell et al., 1999b, 2002).

It is intriguing that sodium channel modulation by both PKA and PKC is voltage dependent and synergistic (Li et al., 1993; Cantrell et al., 1999a, 2002). These results suggest that both PKA and PKC may alter channel function by a similar molecular mechanism, which involves an alteration in voltage-dependent gating. However, no consistent effect of protein phosphorylation on voltage-dependent activation or fast inactivation has been observed. By careful comparison of slow inactivation with neuromodulation by PKA and PKC in cortical neurons and transfected cells, Carr et al. (2003) showed a close correlation between these processes and suggested that neuromodulation by PKA and PKC may act by enhancing the intrinsic slow inactivation process of sodium channels.

*Correspondence: wcatt@u.washington.edu

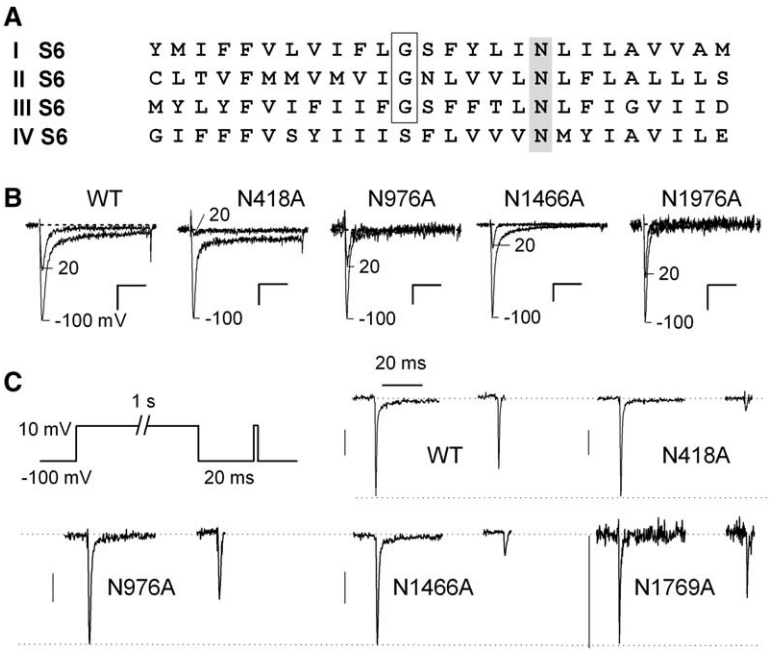

Figure 1. Effects of Mutation of Conserved Asparagine Residues in the S6 Segments on Slow Inactivation

(A) Amino acid sequences of the S6 segments of rat $Na_V1.2a$ channels. The glycine hinge (G) and the conserved asparagine residues (N) in S6 segments are highlighted.

(B and C) Slow inactivation of wild-type (WT) and mutant $Na_V1.2a$ channels. (B) From a holding potential of −100 mV, a 20 ms test pulse was applied alone (−100 mV) or preceded by a 1 s prepulse to +20 mV and a 20 ms period at the holding potential of −100 mV to allow recovery from fast inactivation. Currents recorded during the test pulses without (−100) and with (20) prepulses are superimposed for each mutant channel. (C) (Inset) A prepulse to 10 mV for 1 s was applied, the cells were repolarized to −100 mV for 20 ms to allow recovery of fast inactivation, and a test pulse to 10 mV for 2 ms was applied, and sodium currents were measured. The records show the sodium current during the first 30 ms of the prepulse and during the test pulse for WT and the indicated mutants. Scale bars: 5 ms, 500 pA (B); 20 ms, 500 pA (C).

In this study, we have identified a critical, highly conserved amino acid residue required for slow inactivation, asparagine 1466 in transmembrane segment S6 in domain III. Mutations at this position can increase or nearly completely prevent slow inactivation, identifying this highly conserved asparagine residue in the S6 segments as a crucial molecular determinant of slow inactivation. Using these novel mutants, we show that slow inactivation is in fact required for neuromodulation of sodium channels by PKA and PKC. Our results shed new light on the molecular mechanism of slow inactivation and show that it is the mechanism by which neuromodulation of sodium channels alters autonomous and synaptically driven activity in central neurons.

Results

Single Amino Acid Mutations that Alter Slow Inactivation

The pore-forming α subunits of sodium channels consist of four domains (I–IV), which each contain six transmembrane segments (S1 to S6; Catterall, 2000). The P loops between the S5 and S6 segments line the narrow outer mouth of the pore, while the inner pore lining is formed by the S6 segments. Bending of the S6 segments at a hinge glycine residue is thought to open the pore of potassium channels (Jiang et al., 2002a, 2002b), and forced bending of the S6 segments at this position by substitution of a proline greatly increases activation and prevents slow inactivation of a bacterial sodium channel (Zhao et al., 2004b). Because slow inactivation is a conserved property of all sodium channels, we reasoned that mutation of highly conserved amino acid residues in the S6 segments of mammalian sodium channels might alter slow inactivation without major changes in other sodium channel properties. Such mutants would add to our understanding of the molecular basis for slow inactivation and would provide a substrate for tests of the role of slow inactivation in neuromodulation.

Only one amino acid residue is conserved in the S6 segments of all four domains in all mammalian sodium channels—an asparagine at position 18 in the α helix located six positions downstream of the hinge glycine (Figure 1A). Review of our previous studies of alanine-substitution mutations in the drug-binding sites in the S6 segments (Yarov-Yarovoy et al., 2002) suggested increased slow inactivation for the mutation of N1466 in domain III of the rat brain $Na_V1.2$ channel, and mutation at the corresponding position in the S6 segment of domain I of the skeletal muscle $Na_V1.4$ channel (N434) also altered slow inactivation (Wang and Wang, 1997; Nau et al., 1999).

To investigate the potential role of these highly conserved asparagine residues in slow inactivation, we first mutated each to alanine in $Na_V1.2$ (N418A, N976A, N1466A, and N1769A) and studied them by whole-cell voltage-clamp recording. Slow inactivation was measured without contamination from fast inactivation by using the protocol illustrated in Figures 1B and 1C. An inactivating prepulse to 20 mV (Figure 1B) or 10 mV (Figure 1C) was applied for 1 s, the cells were briefly repolarized to −100 mV to reverse fast inactivation, and sodium currents were measured during a second test pulse to 10 mV for 20 ms (Figure 1B) or 2 ms (Figure 1C). As previously reported by many investigators (eg., Carr et al., 2003, for brain sodium channels), the transient sodium current has similar kinetics before and after the prepulse that induces slow inactivation, but the peak sodium current is reduced in the second test pulse as sodium channels become unavailable for activation (Figure 1B). The sodium current in the second pulse was reduced for wild-type and all mutants, but the reduction was much greater for mutants N418A and N1466A (Figures 1B and 1C). We used the voltage-clamp protocol of Figure 1C with 2 ms test pulses for further analysis of the kinetics of slow inactivation in these mutants.

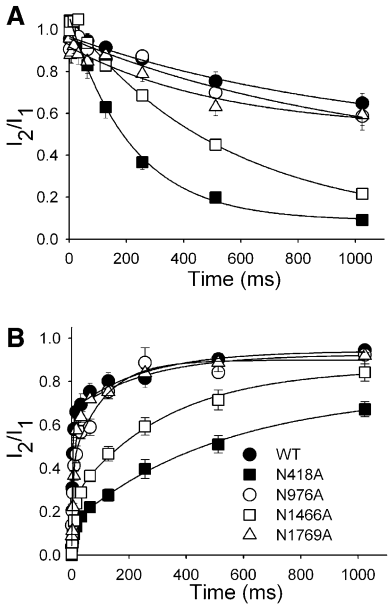

Figure 2. Effects of Mutations at the Conserved Asparagine Residues in the S6 Segments on the Onset and Recovery from Slow Inactivation

(A) Onset of slow inactivation. From a holding potential of −100 mV, a test pulse to 10 mV for 10 ms was applied, and the peak sodium current was measured (I_1). A prepulse to 10 mV for the indicated times was then applied, the cells were repolarized to −100 mV for 20 ms to allow recovery of fast inactivation, a second test pulse to 10 mV for 10 ms was applied, and peak sodium currents (I_2) were measured for WT and the indicated mutants. The data at different prepulse durations were fit with a single exponential.

(B) Recovery from slow inactivation. From a holding potential of −100 mV, a test pulse to 10 mV for 10 ms was applied and the peak sodium current was measured (I_1). A prepulse to 10 mV for 1 s was then applied, the cells were repolarized to −100 mV for the indicated times to allow recovery from inactivation, a second test pulse to 10 mV for 2 ms was applied, and peak sodium currents were measured (I_2) for WT and the indicated mutants. The ratio of peak amplitude of sodium current evoked in the second test pulse to that evoked in the first test pulse is plotted against the duration of interpulse duration and fit to a single exponential.

Scale bars: 2 ms, 500 pA for N1466A and 2 ms, 200 pA for N1466D (A); 4 ms, 500 pA (B). Error bars represent SEM.

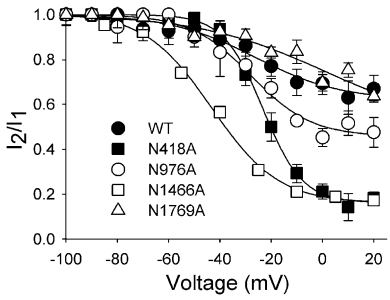

Figure 3. Voltage Dependence of Slow Inactivation of Sodium Channels with Mutations in the Conserved Asparagine Residues in the S6 Segments

From a holding potential of −100 mV, a test pulse to 10 mV for 10 ms was applied and the sodium current (I_1) was measured. A prepulse to the indicated potentials was then applied for 1 s, the cells were repolarized to −100 mV for 20 ms to allow recovery of fast inactivation, a second test pulse to 10 mV for 10 ms was applied, and peak sodium currents (I_2) were measured for WT and the indicated mutants. The ratios of peak sodium currents after and before the prepulse (I_2/I_1) were plotted against the voltage of the conditioning pulse, and the data were fit to the Boltzmann equation. WT, V_s = −28.1 ± 7.3 mV, k = 12.9 ± 1.2 (n = 4); N418A, V_s = −23.3 ± 2.5 mV, k = 7.6 ± 0.4 (n = 4); N967A, V_s = −30.0 ± 4.6 mV, k = 10.1 ± 2.4 (n = 6); N1466A, V_s = −43.4 ± 1.2 mV, k = 13.0 ± 0.7 (n = 5). V_s and k values were not estimated for N1769A because of the low extent of slow inactivation. Error bars represent SEM.

We measured the rate of onset of slow inactivation by varying the duration of the inactivating prepulse (Figure 2A) and the rate of recovery by varying the duration of repolarization to −100 mV following a 1 s inactivating prepulse (Figure 2B). Mutants N418A and N1466A inactivated more rapidly and completely and recovered more slowly than wild-type, while N976A and N1769A were unchanged. These results indicate that mutation of the conserved asparagine residues in the S6 segments of domains I and III to alanine increases slow inactivation while mutation of those in domains II and IV does not.

We measured the voltage dependence of slow inactivation by varying the voltage during the inactivating prepulse from −100 mV to +20 mV in 10 or 15 mV increments (Figure 3). Mutation N1466A caused the largest negative shift in the voltage dependence of slow inactivation. The voltage for half-maximal slow inactivation, V_s, was negatively shifted to −43.4 ± 1.2 mV (n = 5) compared to wild-type (−28.1 ± 7.3 mV, n = 4), and the maximal inhibition of peak current was increased from 34.0% ± 7.0% to 82.0% ± 4.0%. N418A also increased the extent of inactivation to 85.0% ± 2.0%, but did not cause a substantial negative shift in V_s (−23.3 ± 2.5 mV, n = 4). The slope of voltage-dependent inactivation of N418A was very steep, similar to the analogous mutation N434A in the $Na_V1.4$ skeletal muscle sodium channel (Wang and Wang, 1997). In contrast to these strong effects of mutations in domains I and III, mutations N976A in domain II and N1769A in domain IV had only modest effects on the voltage dependence of slow inactivation.

Opposite Effects of Different Amino Acid Substitutions for N1466

Mutation of N1466 to alanine increased the hydrophobicity at position 1466 and increased slow inactivation. Therefore, we substituted the negatively charged amino acid residue aspartate to determine whether an increase in charge and hydrophilicity at that position would prevent slow inactivation. As a first step in analyzing mutant N1466D, we determined the voltage dependence of activation and fast inactivation and compared them to wild-type and N1466A (Figure 4). To measure activation, cells were depolarized from −100 mV to the indicated voltages for 20 ms, and sodium currents were measured. The voltage for half-maximal activation (V_a) of N1466A was −11.4 ± 1.2 mV (n = 11), only slightly shifted to more positive potentials from wild-type (V_a = −14.9 ± 3.7 mV, n = 7). V_a for N1466D was −16.9 ± 2.2 mV (n = 13), not significantly different from wild-type. The voltage dependence of fast inactivation was examined by depolarizing cells to the indicated prepulse potentials for 100 ms from a holding potential of −100 mV and then applying a test pulse to 10 mV for 20 ms to measure sodium currents. The voltage for half-maximal fast inactivation,

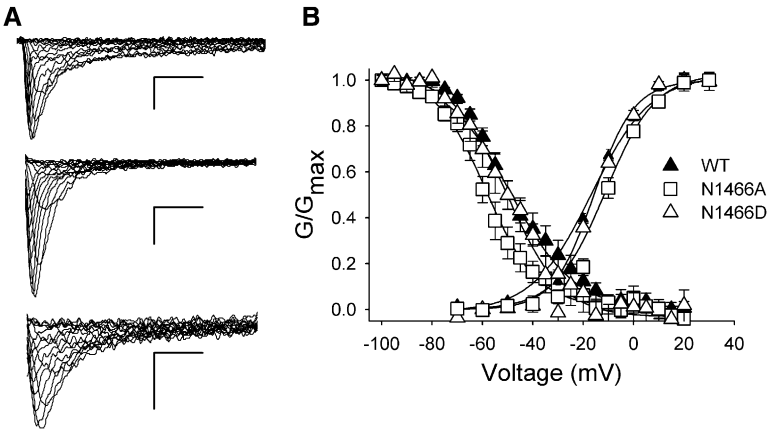

Figure 4. Voltage Dependence of Activation and Fast Inactivation of Mutants at N1466

(A) Representative sodium current traces for activation of sodium currents measured as in panel (B). WT (top), N1466A (middle), and N1466D (bottom). Scale bars: 2 ms, 500 pA.

(B) Activation. From a holding potential of −100 mV, a test pulse to the indicated potentials for 10 ms was applied and the sodium current was measured. Conductance was calculated from the peak sodium current and the extrapolated reversal potential as described in Experimental Procedures. WT, V_a = −14.9 ± 3.7 mV, k = 6.8 ± 0.6 (n = 7); N1466A, V_a = −11.4 ± 1.2 mV, k = 6.4 ± 0.3 (n = 11); N1466D, V_a = −16.9 ± 2.2 mV, k = 8.0 ± 0.4 (n = 13). Fast inactivation. From a holding potential of −100 mV, a prepulse to the indicated potentials was applied for 100 ms, a test pulse to 10 mV for 10 ms was applied, and sodium currents were measured for WT and the indicated mutants. The current in the test pulse was normalized to that recorded at the most negative prepulse potential and plotted versus the potential of the prepulse. WT, V_h = −48.8 ± 0.8 mV, k = 9.5 ± 0.7 (n = 6); N1466A, V_h = −59.6 ± 2.8 mV, k = 8.5 ± 0.7 (n = 11); N1466D, V_h = −50.9 ±1.7 mV, k = 10.0 ± 0.6 (n = 8). Error bars represent SEM.

V_h, of N1466A was −59.6 ± 2.8 mV (n = 11), significantly more negative than for wild-type (V_h = −48.8 ± 0.8 mV, n = 7). V_a for N1466D was −50.7 ± 1.7 mV (n = 13), not significantly different from wild-type. Overall, these mutations at N1466 have only small effects on activation and fast inactivation and therefore may be useful for analysis of the mechanism of slow inactivation and assessment of its role in neuromodulation.

In contrast to their minor effects on activation and fast inactivation, the N1466A and N1466D had major, opposite effects on slow inactivation. N1466D reduced slow inactivation, such that no significant slow inactivation was observed in 1 s prepulses (Figure 5A). In contrast, sodium current through wild-type channels was reduced by slow inactivation with a time constant (τ_s) of 1473 ± 379 ms (n = 8), whereas slow inactivation of N1466A was substantially increased and had a mean τ_s value of 549 ± 40 ms (n = 8, $p < 0.05$).

Recovery from inactivation was measured by depolarizing to 10 mV for 1s to allow both fast and slow inactivation, followed by repolarization to −100 mV for the indicated time periods to allow recovery (Figure 5B). Wild-type sodium channels recovered from inactivation in a two-exponential time course representing fast and slow inactivation, respectively. The fast-inactivated channels (68% of total) recovered with τ = 3.9 ± 0.3 ms, whereas slow inactivated channels (32% of total) recovered with τ = 203 ± 35 ms. Recovery from inactivation for mutant N1466D was much faster and followed a single-exponential time course (τ = 3.1 ± 0.2 ms; Figure 5B), consistent with this channel entering only the fast-inactivated state in 1 s depolarizations. This result is expected from the lack of slow inactivation in 1 s prepulses in Figure 5A. Recovery of mutant N1466A from inactivation was fit by time constants of 3.9 ± 0.3 ms and 241 ± 55 ms (n = 6), similar to wild-type. However, a much larger fraction of channels (74%) recovered from the slow-inactivated state (Figure 5B), consistent with increased entry into the slow-inactivated state in this mutant (Figure 5A).

The voltage dependence of slow inactivation was assessed with the use of a 5 s depolarizing prepulse to allow wild-type sodium channels to approach steady-state slow inactivation (Figure 5C). Maximal inhibition of sodium current through N1466D channels (17.3% ± 0.4%, n = 5) was much less than for wild-type (64.9% ± 0.3%, n = 5). Conversely, N1466A had a larger maximal reduction of sodium current during 5 s prepulses (92.8% ± 0.2%, n = 7) and negatively shifted voltage dependence of inactivation (V_s = −61.9 ± 1.3 mV) compared to wild-type (V_s = −33.1 ± 4.0 mV, n = 5, $p < 0.01$). Altogether, these results implicate N1466 as a crucial molecular determinant of slow inactivation, whose replacement by selected amino acid residues can lead to either markedly increased or markedly inhibited slow inactivation without other major effects on voltage-dependent gating. These results implicate these conserved asparagine residues at position 18 in the S6 segments as crucial molecular elements in the pathway of slow inactivation.

Neuromodulation of Mutants N1466A and N1466D by PKA and PKC

If neurotransmitters that act through PKA and PKC cause voltage-dependent reduction in sodium channel availability by enhancing slow inactivation as proposed (Carr et al., 2003), we would expect that the effects of PKA and PKC would be increased by the N1466A mutation and would be prevented by the N1466D mutation. 1-Oleoyl-2-acetyl-sn-glycerol (OAG), an analog of the PKC activator diacylglycerol, mimics the actions of neurotransmitters on sodium channels in neurons and has been used extensively to study PKC modulation of sodium channels in neurons and transfected cells (Cantrell et al., 1996, 2002; Carr et al., 2003; Chen et al., 2005; Dascal and Lotan, 1991; Numann et al., 1991; Sigel and Baur, 1988; West et al., 1991). In order to measure voltage-dependent modulation by PKC, we maintained cells at a holding potential of −70 mV while perfusing 50 μM OAG and recorded sodium currents during 20 ms test pulses to +10 mV applied every 20 s. As in previous experiments in neurons and transfected cells (Cantrell et al., 1996, 2002), peak sodium currents through wild-type sodium channels declined by 27.8% ± 3.3% over 3.7 min (Figure 6A). The decline of sodium current was

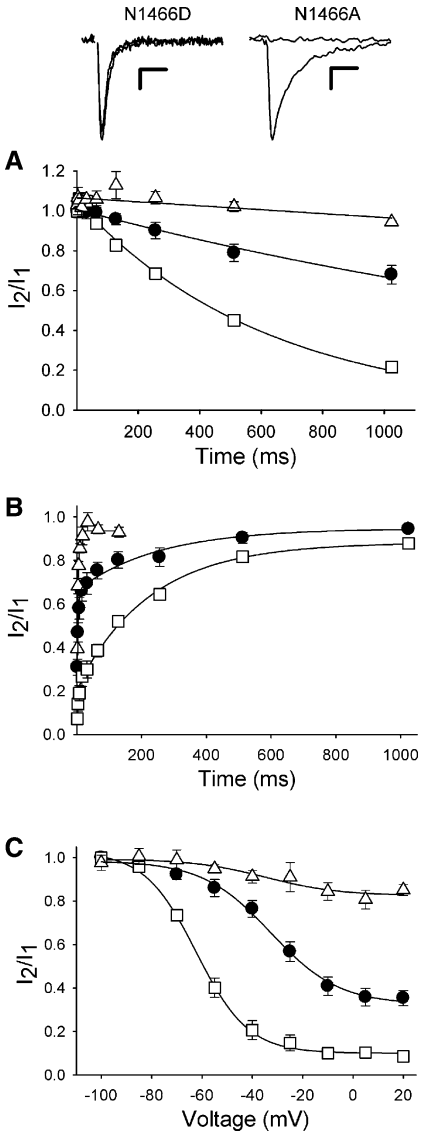

Figure 5. Kinetics of Slow Inactivation for Mutants at N1466

Sodium current records at top illustrating the differing degrees of slow inactivation in N1466D channels (left) and N1466A channels (right). Currents were recorded during test pulses to +10 mV without and with a preceding 5 s long pulse to +20 mV and a 20 ms repolarization to −100 mV (see panel [C]). Scale bars: 2 ms, 500 pA. (A) Onset of slow inactivation. From a holding potential of −100 mV, a test pulse to 10 mV for 10 ms was applied and the sodium current was measured. A prepulse to 10 mV was then applied for the indicated durations, the cells were repolarized to −100 mV for 20 ms to allow recovery of fast inactivation, a second test pulse to 10 mV for 10 ms was applied, and sodium currents were measured for WT and the indicated mutants. WT, τ = 1473 ± 379 ms (n = 8). N1466A, τ = 549 ± 40 ms (n = 8). N1466D, no significant slow inactivation at 1 s (n = 8). (B) From a holding potential of −100 mV, a test pulse to 10 mV for 10 ms was applied and the peak sodium current was measured (I_1). A prepulse to 10 mV was then applied for 1 s, the cells were repolarized to −100 mV for the indicated time intervals to allow recovery from inactivation, a second test pulse to 10 mV for 2 ms was applied, and the peak sodium current was measured (I_2) for WT and the indicated mutants. The ratios of test pulse currents are plotted versus prepulse duration. Recovery from inactivation of WT and N1466A was best described by two exponential components: WT, τ_1 = 9.7 ± 0.3 ms; τ_2 = 590.1 ± 94 ms; N1466A, τ_1 = 3.9 ± 0.3 ms; τ_2 = 241 ± 56 ms. The N1466D data were fit with a single exponential of 3.1 ± 0.2 ms. (C) From a holding potential of −100 mV, a test pulse to 10 mV for 10 ms was applied and the sodium current was measured. A prepulse to the indicated potentials was then applied for 5 s, the cells were repolarized to −100 mV for 20 ms to allow recovery of fast inactivation, a second test pulse to 10 mV for 10 ms was applied, and sodium currents were measured for WT (circles), N1466A (squares), and N1466D (triangles) and the indicated mutants. WT, V_s = −33.1 ± 4.0 mV, k = 13.0 ± 1.5, S_{max} = 64.9% ± 0.3% (n = 5); N1466A, V_s = −61.9 ± 1.3 mV, k = 11.1 ± 1.8, S_{max} = 92.8% ± 0.2% (n = 7); N1466D, S_{max} = 17.3% ± 0.4% (n = 5). V_s and k were not estimated quantitatively for N1466D because of the small extent of slow inactivation. Error bars represent SEM.

much faster for mutant N1466A (Figure 6A). In contrast to the increased slow inactivation of N1466A, OAG did not cause a significant decline in sodium current for mutant N1466D (5.5% ± 3.6%; Figure 6A). These results provide strong support for the conclusion that neuromodulation reduces sodium channel availability by activation of PKC and consequent enhancement of slow inactivation. If slow inactivation is blocked, the effect of PKC activation is completely lost. Conversely, if slow inactivation is increased, the effect of PKC activation is also increased.

In the experiments of Figure 6A, we have used −70 mV as a holding potential to mimic neurons near the threshold for slow inactivation, and we have normalized the sodium currents at the beginning of the experiment to allow quantitative comparison of cells expressing wild-type and mutant channels. However, there is significant slow inactivation at −70 mV for wild-type and substantial slow inactivation at −70 mV for mutant N1466A (Figure 5C). Therefore, the true magnitude of the cumulative effects of slow inactivation at −70 mV plus the enhancement of slow inactivation caused by activation of PKC is diminished by the normalization procedure. To illustrate the full magnitude of these effects, we have adjusted the data for each mutant by a factor reflecting the amount of steady-state slow inactivation at −70 mV as measured in the experiments of Figure 5C and replotted the data in Figure 6B. When the combined effects of slow inactivation and its enhancement by activation of PKC are considered, the sodium current for N1466A is reduced to 56% of maximum, while the sodium current of N1466D remains at essentially 95%. This representation of the results gives a clearer picture of the full dynamic range of regulation of sodium currents by slow inactivation at −70 mV plus its enhancement by activation of PKC for N1466A and wild-type sodium channels and further emphasizes the nearly complete loss of this regulation in the N1466D mutant.

To examine the role of slow inactivation in modulation of sodium channel availability by PKA, we used the membrane-permeant cAMP analog DCl-cBIMPS (cBIMPS) as PKA activator, as in previous experiments in neurons and transfected cells (Cantrell et al., 1997, 1999a; Carr et al., 2003). Using the same protocol as in our experiments on PKC modulation, we found that peak sodium currents through wild-type sodium channels declined by 30.6% ± 3.6% (n = 5) in 9 min in the presence of cBIMPS (Figure 7A). The rate of decline of sodium currents after external perfusion of the cells with cBIMPS was substantially accelerated for N1466A (Figure 7A). In contrast, the sodium currents conducted by N1466D channels did not decline significantly after external perfusion

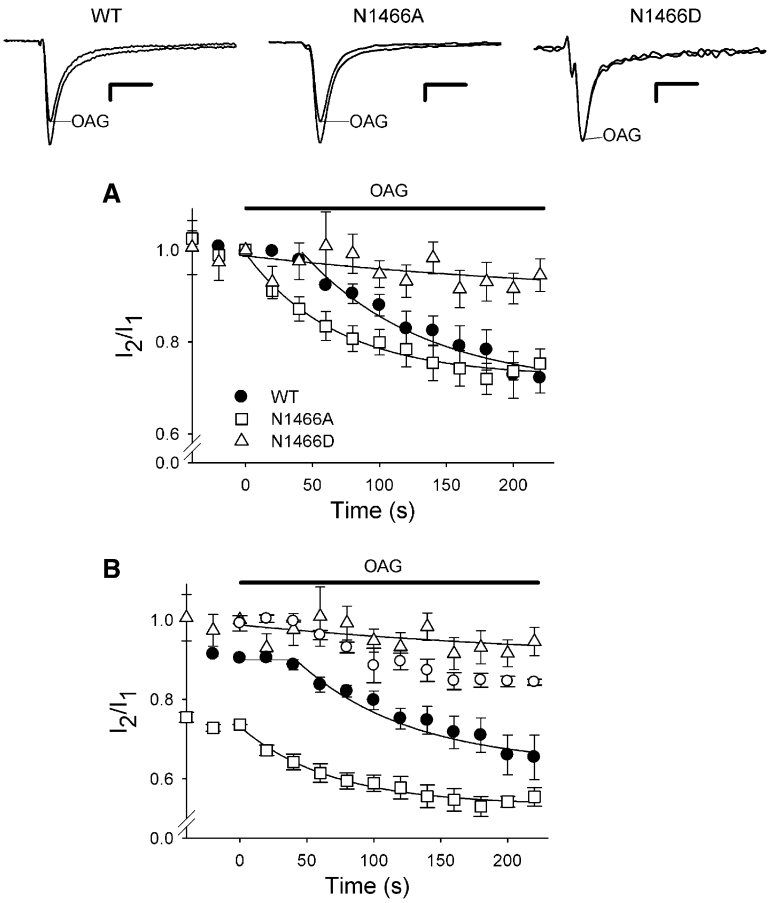

Figure 6. Modulation of Mutants N1466A and N1466D by Activation of PKC

(A) From a holding potential of −70 mV, sodium currents were evoked every 20 s by a 20 ms test pulse to 10 mV. Perfusion with OAG (50 μM) began at 0 s (bar). At 3.7 min, the peak sodium current was reduced as follows: WT, 27.8% ± 3.3%; N1466D, 5.5% ± 3.6%; N1466A, 26.3% ± 1.9%. (Inset) Representative sodium current traces before and after addition of OAG. Scale bars: 2 ms, 500 pA for WT and N1466A; 2 ms, 100 pA for N1466D.

(B) The results of panel (A) were replotted after adjustment for steady-state slow inactivation at −70 mV. Values were multiplied by the level of steady-state slow inactivation at −70 mV for the appropriate mutant channel from the data of Figure 5C.

Error bars represent SEM.

with cBIMPS (5.0% ± 4.3%, n = 9; Figure 7A). As for the PKC experiments, we have replotted these results in Figure 7B, adjusting for the different extents of slow inactivation at the holding potential of −70 mV (see Figure 5C), which further emphasizes the nearly complete loss of both forms of regulation in mutant N1466D. These results provide strong support for the conclusion that neuromodulation reduces sodium channel availability by activation of PKA and consequent enhancement of slow inactivation. We previously observed that a low level of activation of PKC, which had little effect on sodium current, could greatly increase the effect of simultaneous activation of PKA (Li et al., 1993; Cantrell et al., 1999a, 2002). In light of our present results, the synergistic effects of PKC and PKA in modulation of sodium channels likely reflect their common stimulation of the slow inactivation process, providing a final common, voltage-dependent pathway to sodium channel modulation.

A Biophysical Model for Slow Inactivation and Neuromodulation of Sodium Channels

The reduction in sodium channel availability observed in our experiments reflects a series of events—activation of PKA or PKC, phosphorylation of the site(s) on the sodium channel required for regulation, and conversion of sodium channels into the slow inactivated state, making them unavailable for activation. Previous studies have identified multiple sites of phosphorylation that are involved in modulation of sodium channels by PKA and PKC (Murphy et al., 1993; Smith and Goldin, 1997; Cantrell et al., 1997, 2002). It is likely that the rates of action of PKA and PKC on sodium channels are controlled by activation of the kinases and phosphorylation of the sodium channel, because the rate of reduction of sodium channel availability following activation of PKA and PKC (Figures 6 and 7) is more than 10-fold slower than the rate of slow inactivation (Figure 5A). We used a biophysical model of the slow inactivation process (Carr et al., 2003) to predict the unknown rate of slow inactivation that would occur *after* the biochemical processes are complete and to fit the measured extents of reduction of sodium channel availability of the wild-type and mutant sodium channels (Figure). The rates for entry into the slow inactivated state were measured in experiments like those illustrated in Figure 5A, extended to 20 s for mutant N1446D to allow detectable slow inactivation. These data were used to adjust the rate constant $\alpha 2$ (Figure 8A) controlling entry from the fast inactivated state (I6) to the slow inactivated state (IS2). With these experimentally derived rate constants, the model closely reproduced the voltage dependence of slow inactivation in 5 s prepulses from Figure 5C (Figure 8B). This close fit indicates that this simple model provides an accurate description of slow inactivation under the conditions of these experiments, but we suspect that more complex kinetic models may be needed to fully describe slow inactivation over a wider range of times and test voltages.

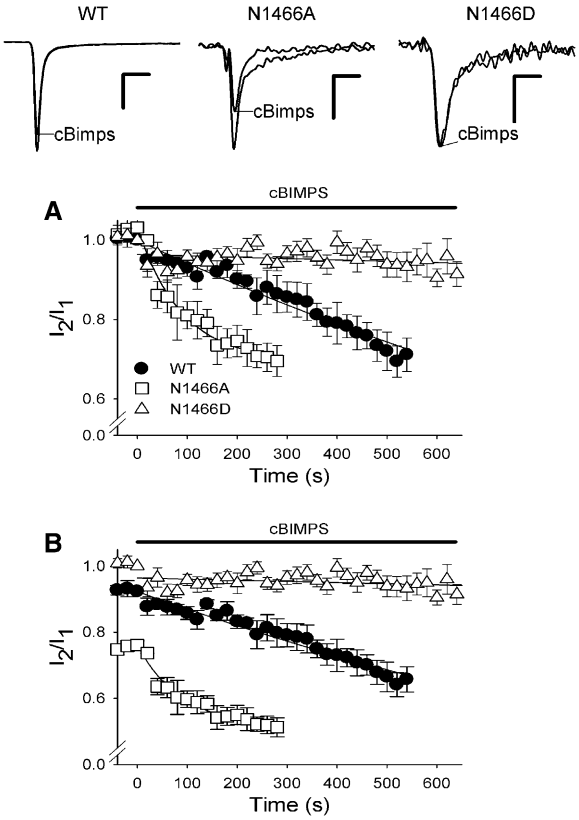

Figure 7. Modulation of Mutants N1466A and N1466D by Activation of PKC

(A) From a holding potential of −70 mV, sodium currents were evoked every 20 s by a 20 ms test pulse to 10 mV. Perfusion with cBIMPS (50 μM) began at 0 s (bar). The peak sodium current was reduced as follows: WT, 30.6% ± 3.9% at 600 s, n = 5; N1466D, 5.0% ± 4.3% at 560 s, n = 9; N1466A, 29.5% ± 3.6% at 300 s (n = 5). (Inset) Representative sodium current traces before and after addition of cBIMPS. Scale bars: 2 ms, 200 pA.

(B) The results of panel (A) are replotted after adjustment for the steady-state slow inactivation at −70 mV using the results of Figure 5C.

Error bars represent SEM.

The effect of phosphorylation was introduced into the model as adjustments of the rate constant $\alpha 2$ controlling slow inactivation in order to produce the time courses illustrated in Figure 8C. As expected, the rates of reduction of sodium channel availability by slow inactivation are much faster than observed in our experiments (Figures 6 and 7) because they represent the slow inactivation process *after* completion of sodium channel phosphorylation. The extents of reduction of sodium channel availability approximate those observed in the experiments presented in Figures 6B and 7B. A 2-fold change in rate constant by "phosphorylation" in the model was sufficient to fit the data for N1446A, whereas a 67-fold change in rate constant by "phosphorylation" was required to approximately fit the data for wild-type. No effect of "phosphorylation" was observed for a 67-fold change (data not shown) or even a 100-fold change (Figure 8C) in rate constant for N1446D. We speculate that the 2-fold change in rate constant required to reproduce the effect of "phosphorylation" of N1446A in the model may reflect the effect of phosphorylation of only one of the multiple sodium channel phosphorylation sites (Murphy et al., 1993; Cantrell et al., 2002), which is sufficient to further enhance slow inactivation of this mutant that has an increased rate of slow inactivation under baseline conditions. In contrast, phosphorylation of two or more sites may be needed to give the 67-fold change in rate constant needed to approximate the effect of phosphorylation on wild-type sodium channels, and even this level of phosphorylation is not sufficient to enhance the slow inactivation of N1446D channels that have impaired slow inactivation.

Discussion

Sodium Channels, Slow Inactivation, and Cellular Neuroplasticity

Neuromodulation of sodium channels plays an important role in cellular neuroplasticity (reviewed in Cantrell and Catterall, 2001). In pyramidal neurons from the prefrontal cortex, activation of 5-HT2a/c receptors acts through PKC to increase threshold for action potential firing and shorten trains of action potentials, and these actions reflect primarily a reduction in sodium channel availability (Carr et al., 2002, 2003). In striatal medium spiny neurons, regulation of sodium channels by dopamine acting through D1 and D2 receptors, PKA, and PKC contributes to the transitions between the up and down states of cell firing (Surmeier and Kitai, 1997). In striatal aspiny cholinergic interneurons, dopamine acts through D2 receptors and PKC to reduce sodium channel availability and slow pacemaking (Maurice et al., 2004). As these examples illustrate, neuromodulation of sodium channels has a major influence on the input-output relationships of diverse CNS neurons.

Neuromodulation of sodium channels mediated by PKA and PKC in hippocampal and cortical pyramidal neurons is voltage dependent (Cantrell et al., 1999a; Carr et al., 2003). In spite of the striking voltage dependence of PKA and PKC actions, activation of these protein kinases does not have a consistent, large effect on the voltage dependence or kinetics of sodium channel activation or fast inactivation. Phosphorylation of the channel itself does not appear to be voltage dependent; however, recent work has shown a close correlation of the onset, voltage dependence, and recovery of neuromodulation by PKA and PKC with the onset, voltage dependence, and recovery of slow inactivation, an important intrinsic gating process of sodium channels that controls sodium channel availability (Carr et al., 2003). The hypothesis advanced in our present work is that voltage dependence of the PKA and PKC effects arises because channel phosphorylation affects channel availability by promoting slow inactivation.

Mechanism of Slow Inactivation

Slow inactivation, discovered initially in squid giant axon (Rudy, 1978), is a separate physiological and molecular process from fast inactivation, and these two processes appear to compete with each other for inactivation of sodium channels (Featherstone et al., 1996, Vedantham and Cannon, 1998; Vilin et al., 2001). Fast inactivation and its reversal occur in milliseconds, while slow inactivation and reversal occur in seconds. Mutagenesis

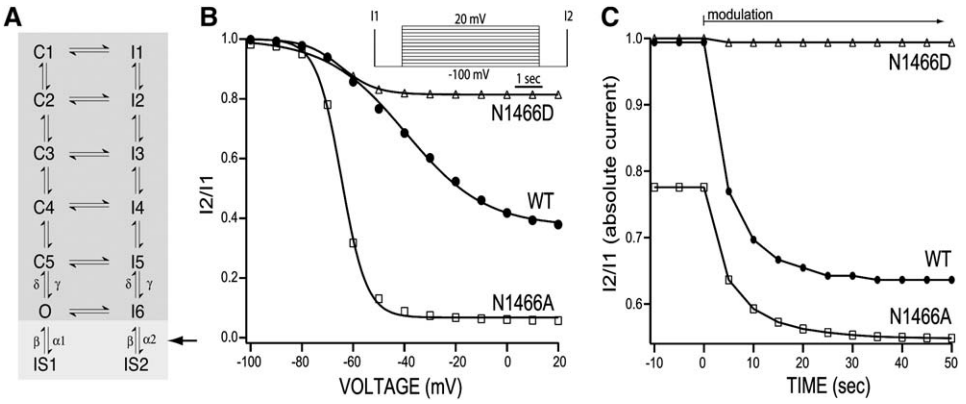

Figure 8. Model for the Effects of Mutations on the Action of Phosphorylation through Slow Inactivation

(A) The topology of the Na^+ channel model used to simulate WT, N1466A, and N1466D channel gating. The models differed only in the forward rate constant ($\alpha 2$) from I6 to IS2.

(B) Plot of the I2/I1 ratio of currents evoked in each of the models by the protocol used in Figure 5C. Data points were fit with modified Boltzmann functions.

(C) Plot of relative current evoked by a brief step to 0 mV from a holding potential of −70 mV in each of the models before and after "phosphorylation." Phosphorylation was mimicked by increasing $\alpha 2$. Increasing $\alpha 2$ of the WT channel by a factor of 67 gave a maximum modulation like that seen in Figures 6 and 7. In contrast, increasing $\alpha 2$ by only a factor of 2 was necessary to mimic the N1466A data. Lastly, increasing $\alpha 2$ by a factor of 100 (or more) failed to result in a significant increase in slow inactivation of the N1466D model.

studies have shown that several sodium channel domains are involved in slow inactivation, including the S4 voltage sensor and adjacent residues (Kontis and Goldin, 1997; Mitrovic et al., 2000), the P region (Cummins and Sigworth, 1996; Balser et al., 1996; Todt et al., 1999; Vilin et al., 1999; 2001; Xiong et al., 2003), and the S6 segments (Wang and Wang, 1997, Nau et al., 1999, O'Reilly et al., 2001; Vedantham and Cannon, 2000). However, previous mutations that have been shown to alter slow inactivation have only partial effects, and there is no accepted model for the mechanism of slow inactivation. For example, although the P region has been suggested to be involved in slow inactivation, chemical modification studies have shown that amino acid residues within it do not move in concert with slow inactivation (Struyk and Cannon, 2002).

The first mutation shown to completely block slow inactivation on the timescale of several seconds was substitution of proline for the hinge glycine residue in the S6 segment of the bacterial sodium channel NaChBac (Zhao et al., 2004b). These experiments showed that mutations that alter the gating movements of S6 segments can completely block slow inactivation, in addition to their dramatic effects on the voltage dependence and polarity of activation gating (Zhao et al., 2004a, 2004b). Conformational changes in the IVS6 segment of skeletal muscle $Na_V1.4$ channels that are proposed to be associated with slow inactivation have also been detected by chemical modification studies (Vedantham and Cannon, 2000). Because slow inactivation is a highly conserved process, it is likely that highly conserved amino acid residues are involved. The most highly conserved amino acid residue in the S6 segments of sodium channels is the asparagine at position 18. Our results show that this amino acid residue is indeed crucial for slow inactivation. Mutation to a more hydrophobic residue (alanine) increases slow inactivation, whereas mutation to a more hydrophilic residue (aspartic acid) completely prevents slow inactivation during 5 s depolarizations. These results add a new dimension to studies of the molecular mechanism of slow inactivation by showing that single amino acid mutations in the S6 segments can completely block slow inactivation without other effects on sodium channel gating. These results, plus the previous chemical modification and proline substitution studies (Vedantham and Cannon, 2000; Zhao et al., 2004a, 2004b), implicate gating movements of the S6 segments involving their uniquely well-conserved asparagine residues in position 18 in the gating transitions that lead to slow inactivation. Further studies of this region of the sodium channel should lead to additional insights into the molecular mechanism of the slow inactivation gating process.

Neuromodulation of Sodium Channels by PKA and PKC Enhances Slow Inactivation

Our results bring together two extensive lines of research—studies of the role of slow inactivation in control of neuronal excitability and studies of the role of neurotransmitter-activated protein phosphorylation in control of sodium channel function. As reviewed in the Introduction, sodium channels are phosphorylated by PKA and PKC in response to neurotransmitter activation of G protein-coupled receptors. This phosphorylation reduces sodium channel availability in a synergistic manner (Li et al., 1993; Cantrell et al., 2002), but only at depolarized voltages where neurons are spiking, endowing this modulation with an activity dependence that is unique among neuromodulatory events. The activity-dependent reduction in sodium channel availability produced by phosphorylation leads to slowing of autonomous, sodium channel-driven spiking, to elevation in spike threshold, and to alterations in synaptically driven spiking patterns. The voltage dependence of neuromodulation by PKA and PKC (Cantrell et al., 1999a; Carr et al., 2003) led to the hypothesis that these protein kinases may act by enhancing slow inactivation (Carr et al., 2003). Comparison of the time of onset, the voltage

dependence, and the time for recovery from neuromodulation with the same parameters for slow inactivation revealed a close correlation (Carr et al., 2003). Our present results establish that neuromodulation of sodium channels by PKA and PKC causes enhanced slow inactivation, which is both necessary and sufficient for their effects on sodium currents. Mutation of one asparagine residue to alanine in the S6 segment increased slow inactivation and modulation by PKA and PKC, whereas changing this residue to aspartate impaired slow inactivation and prevented modulation. These results strongly support a model in which neuromodulation by PKA and PKC is caused by enhancement of the intrinsic slow inactivation gating process.

A Kinetic Model Predicts the Effects of Mutation, Slow Inactivation, and Phosphorylation

Although we lack information on the kinetics of the phosphorylation process itself, we found it useful to model the changes in slow inactivation resulting from protein phosphorylation that were required to reproduce our results. To do this, we extended a kinetic model developed previously (Carr et al., 2003) by increasing (for N1466A) or decreasing (for N1466D) the rate constant, $\alpha 2$, governing the transition from the last fast inactivated state, I6, to the slow inactivated state, IS2. We found that this model fit our slow inactivation results for wild-type and mutants well and that the effects of phosphorylation were mimicked by increasing the rate of entry into the slow inactivated state. These results further support the conclusion that neuromodulation by protein phosphorylation acts through enhancement of slow inactivation.

Previous studies showed that modulation of sodium channels by PKA and PKC is synergistic—low-level activation of one pathway increases the effectiveness of the other (Li et al., 1993). Partially overlapping sets of phosphorylation sites in the intracellular loop between domains I and II are involved in the individual effects of each kinase and in their synergy (Cantrell et al., 2002). The discovery that both PKA and PKC enhance slow inactivation provides a conceptual framework for understanding the synergistic interaction of these regulatory pathways and their activity dependence. As both pathways enhance slow inactivation, it is expected that partial activation of one pathway will increase the effects of the other. Moreover, as slow inactivation is induced by sustained membrane depolarization, it is clear why the effects of both the PKA and PKC modulatory pathways are voltage dependent. This highly interactive regulatory network allows the availability of sodium channels for activation to be closely regulated in an integrative manner by prolonged or repetitive membrane potential changes, neurotransmitter activation of PKC, and neurotransmitter activation of PKA.

A Plausible Molecular Mechanism for Enhancement of Slow Inactivation by Protein Phosphorylation

The molecular pathway by which protein phosphorylation of multiple sites in $L_{I\text{-}II}$ of the sodium channel can enhance slow inactivation gating is unknown, but studies of other forms of ion channel modulation provide hints of possible mechanisms. Activation of a bacterial calcium-activated potassium channel (MthK), a small-conductance calcium/calmodulin-activated potassium channel, and cyclic nucleotide-regulated CNG and HCN channels is driven by binding of the regulatory ligands to the C-terminal domain, which is thought to cause a conformational change and exert a force on the adjacent pore-lining S6 segments to bend them (Schumacher et al., 2001; Jiang et al., 2002a, 2002b; Zagotta et al., 2003). Gating of calcium channels is modulated by binding of magnesium and calcium/calmodulin to the C-terminal domain, just inside of the IVS6 segment (Lee et al., 1999; Brunet et al., 2005), and these effects may also derive from a conformational change that exerts force on the IVS6 segment and alters the energetics of its bending. Collectively, these results point to modulation of the energetics of bending of the S6 segments by conformational changes in the adjacent intracellular domains as a key mechanism of ion channel gating and its regulation. Our previous results show that concerted bending of the S6 segments is required for slow inactivation of a bacterial sodium channel (Zhao et al., 2004b), and we show here that highly conserved asparagine residues in S6 segments are required for slow inactivation. Therefore, it is likely that slow inactivation may also be affected by conformational changes in the intracellular domains adjacent to the S6 segments of sodium channels. We suggest that phosphorylation of sites in $L_{I\text{-}II}$ may cause a conformational change that reduces the energy barrier for the gating movements of the adjacent IS6 segment that are required for slow inactivation. By reducing the energy required for IS6 gating movements, phosphorylation by PKA, PKC, or both may enhance slow inactivation and thereby reduce sodium channel availability. Further structure-function studies will be required to test this molecular model.

Experimental Procedures

Molecular Biology, Transfection, and Cell Culture

Plasmid pCDM8-rIIA containing the cDNA encoding the full-length, wild-type rat $Na_V1.2a$ α subunit (Linford et al., 1998) and the asparagine to alanine mutations in each S6 transmembrane segments of the rat $Na_V1.2a$ channel (N418A, N976A, N1466A, N1769A) have been described previously (Ragsdale et al., 1994; Yarov-Yarovoy et al., 2001, 2002). Mutation of domain III asparagine to aspartate (N1466D) was performed using two step, overlap polymerase chain reaction, and subsequently cloned into pCDM8-rIIA utilizing the unique sites, BlpI and BstEII. Fidelity of sequence between these restriction endonuclease sites was verified by DNA sequencing.

TsA-201 cells, a subclonal line of human embryonic kidney HEK293 cells, were maintained as described (Herlitze et al., 1996). Sodium channel expression plasmids were transiently transfected by use of the calcium phosphate coprecipitation method. The cDNA encoding the CD8 receptor in pCD8-NEO was used as a marker of the transfected cells (Margolskee et al., 1993). Twelve hours later, transfected cells were replated at low density for electrophysiological recordings. The transfected cells were identified by labeling with CD8-specific antibody-coated microspheres (Dynal, Oslo, Norway).

Electrophysiology

Whole-cell patch-clamp recordings were performed at room temperature by using an Axopatch 200 amplifier (Axon Instruments, Union City, CA). Data were analyzed with Igor Pro 4.0 software. The voltage-clamp data were filtered at 10 kHz and then digitized at 20 μs per point. 80%–90% series resistance compensation was routinely used. Leak and capacitive transients were subtracted using a P/–4 protocol. Whole-cell voltage-clamp experiments were conducted using an intracellular solution containing 100 mM CsAspartate, 1 mM NaCl, 4 mM $MgCl_2$, 10 mM EGTA, 0.5 mM $CaCl_2$,

25 mM phosphocreatine (Tris salt), 2 mM ATP (Na salt), 0.2 mM GTP (Na salt), and 40 mM HEPES with pH adjusted to 7.3 with CsOH. The extracellular solution contained 140 mM NaCl, 10 mM CsCl, 1 mM $CaCl_2$, 1 mM $MgCl_2$, 10 mM HEPES, and 50 mM glucose, pH 7.3.

Data were analyzed using IgorPro (Wave Metrics, Lake Oswego, OR) or SigmaPlot (Jandel Scientific Co., San Rafael, CA). Conductance-voltage (g-V) relationships (activation curves) were calculated from the current-voltage (*I-V*) relationships according to $g = I_{Na}/(V - E_{Na})$, where I_{Na} was the peak Na^+ current measured at potential, *V*, and E_{Na}, the reversal potential estimated from a line fit to the peak currents measured between +20 and +40 mV and extended to the abscissa. Normalized activation and inactivation curves were fit to Boltzmann relationships of the form: $y = 1/\{1 + \exp[(V - V_{a,h})/k]\} + A$, where *y* is normalized g_{Na} or I_{Na}, *A*, the baseline, *V*, the membrane potential, $V_{1/2}$, the voltage of half-maximal activation or inactivation, and *k* is a slope factor. Slow inactivation-voltage curves were fit with a modified Boltzmann equation (Carr et al., 2003; Vilin et al., 2001) of the form: $I/I_{max} = (1 - I_{resid})/((1 + \exp(-(V_m - V_s)/k)) + I_{resid}$, where I_{resid} is the residual fraction of current at the end of the test pulse and *k* is the slope factor. All averaged data are the mean ± SEM. We determined the statistical significance of differences between groups by Student's t test or paired t test. The threshold p value for statistical significance was 0.05.

Kinetic Modeling

Simulations were performed with the use of NEURON (ver. 5.7) (Hines and Carnevale, 2001). The Na^+ channel model topology was as described by Carr et al. (2003). The rate constants were also as described in this study except that Con (the rate constant for the C1 to I1 transition, Figure 8A) was adjusted to 0.01 to fit the gating properties of the heterologously expressed channels. Models of WT, N1466A, and N1466D channels were derived from this canonical model by adjusting the forward rate constant from the fast inactivated state (I6) to the slow inactivated state (IS2). This rate constant is labeled $\alpha 2$ in Figure 8. This rate constant was dependent upon membrane potential (Vm) and given by a Boltzmann equation of the form $\alpha 2 = C1((1 - C2)/(1 - \exp((Vm - Vh)/Vc))) + C2$. For the WT channel $C1 = 6e^{-4}$, $C2 = 5e^{-2}$, Vh = −20 mV, Vc = 15 mV. For the N1466A channel $C1 = 8e^{-3}$, C2 = 0, Vh = −80 mV, Vc = 100 mV. For the N1466D channel $C1 = 1e^{-6}$, C2 = 0, Vh = −60 mV, Vc = 15 mV. The phosphorylation of the channels was mimicked by increasing C1. C1 was increased by a factor of 67 to $4e^{-2}$ for the WT channel, by a factor of 2 for the N1466A channel to $1.6e^{-2}$ and by a factor of 100 for the N1466D channel to $1e^{-4}$. Channel phosphorylation was assumed to be exponential with a time constant of 10 s.

Acknowledgments

This work was supported by National Institutes of Health Research Grant NS15751 to W.A.C., NS34696 to D.J.S., and NIH NRSA NS43065 to Y.C. We wish to thank Joshua Held and Howard Wu for their help with the kinetic simulations and Dr. Daniel Beacham for comments on a draft of the manuscript.

Received: June 17, 2005
Revised: October 7, 2005
Accepted: January 5, 2006
Published: February 1, 2006

References

Balser, J.R. (2002). Inherited sodium channelopathies: novel therapeutic and proarrhythmic molecular mechanisms. Trends Cardiovasc. Med. *11*, 229–237.

Balser, J.R., Nuss, H.B., Chiamvimonvat, N., Perez-Garcia, M.T., Marban, E., and Tomaselli, G.F. (1996). External pore residue mediates slow inactivation in mu-1 rat skeletal muscle sodium channels. J. Physiol. *494*, 431–442.

Brunet, S., Scheuer, T., Klevit, R., and Catterall, W.A. (2005). Modulation of $Ca_V1.2$ channels by Mg^{2+} acting at an EF-hand motif in the COOH-terminal domain. J. Gen. Physiol. *126*, 311–323.

Cannon, S.C. (1996). Sodium channel defects in myotonia and periodic paralysis. Annu. Rev. Neurosci. *19*, 141–164.

Cantrell, A.R., and Catterall, W.A. (2001). Neuromodulation of Na^+ channels: an unexpected form of cellular plasticity. Nat. Rev. Neurosci. *2*, 397–407.

Cantrell, A.R., Ma, J.Y., Scheuer, T., and Catterall, W.A. (1996). Muscarinic modulation of sodium current by activation of protein kinase C in rat hippocampal neurons. Neuron *16*, 1019–1026.

Cantrell, A.R., Smith, R.D., Goldin, A.L., Scheuer, T., and Catterall, W.A. (1997). Dopaminergic modulation of sodium current in hippocampal neurons via cAMP-dependent phosphorylation of specific sites in the sodium channel α subunit. J. Neurosci. *17*, 7330–7338.

Cantrell, A.R., Scheuer, T., and Catterall, W.A. (1999a). Voltage-dependent neuromodulation of Na^+ channels by D1-like dopamine receptors in rat hippocampal neurons. J. Neurosci. *19*, 5301–5310.

Cantrell, A.R., Tibbs, V.C., Westenbroek, R.E., Scheuer, T., and Catterall, W.A. (1999b). Dopaminergic modulation of voltage-gated Na^+ current in rat hippocampal neurons requires anchoring of cAMP-dependent protein kinase. J. Neurosci. *19*, RC21.

Cantrell, A.R., Yu, F.H., Murphy, B.J., Sharp, E.M., Qu, Y., Catterall, W.A., and Scheuer, T. (2002). Molecular mechanisms of convergent regulation of brain Na^+ channels by protein kinase A and protein kinase C. Mol. Cell. Neurosci. *21*, 63–80.

Carr, D.B., Cooper, D.C., Ulrich, S.L., Spruston, N., and Surmeier, D.J. (2002). Serotonin receptor activation inhibits sodium current and dendritic excitability in prefrontal cortex via a protein kinase C-dependent mechanism. J. Neurosci. *22*, 6846–6855.

Carr, D.B., Day, M., Cantrell, A.R., Held, J., Scheuer, T., Catterall, W.A., and Surmeier, D.J. (2003). Transmitter modulation of slow, activity-dependent alterations in sodium channel availability endows neurons with a novel form of cellular plasticity. Neuron *39*, 793–806.

Catterall, W.A. (2000). From ionic currents to molecular mechanisms: The structure and function of voltage-gated sodium channels. Neuron *26*, 13–25.

Chen, Y., Cantrell, A.R., Messing, R.O., Scheuer, T., and Catterall, W.A. (2005). Specific modulation of Na^+ channels in hippocampal neurons by protein kinase C-ε. J. Neurosci. *25*, 507–513.

Colbert, C.M., Magee, J.C., Hoffman, D.A., and Johnston, D. (1997). Slow recovery from inactivation of sodium channels underlies the activity dependent attenuation of dendritic action potentials in hippocampal CA1 pyramidal neurons. J. Neurosci. *17*, 6512–6521.

Costa, M.R.C., and Catterall, W.A. (1984a). Cyclic-AMP-dependent phosphorylation of the a subunit of the sodium channel in synaptic nerve ending particles. J. Biol. Chem. *259*, 8210–8218.

Costa, M.R.C., and Catterall, W.A. (1984b). Phosphorylation of the a subunit of the sodium channel by protein kinase C. Cell. Mol. Neurobiol. *4*, 291–297.

Costa, M.R.C., Casnellie, J.E., and Catterall, W.A. (1982). Selective phosphorylation of the α subunit of the sodium channel by cAMP dependent protein kinase. J. Biol. Chem. *257*, 7918–7921.

Cummins, T.R., and Sigworth, F.J. (1996). Impaired slow inactivation in mutant sodium channels. Biophys. J. *71*, 227–236.

Dascal, N., and Lotan, I. (1991). Activation of protein kinase C alters the voltage-dependence of sodium channel. Neuron *6*, 165–175.

Do, M.T., and Bean, B.P. (2003). Subthreshold sodium currents and pacemaking of subthalamic neurons: modulation by slow inactivation. Neuron *39*, 109–120.

Featherstone, D.E., Richmond, J.E., and Ruben, P.C. (1996). Interaction between fast and slow inactivation in Skm1 sodium channels. Biophys. J. *71*, 3098–3109.

Gonzalez-Burgos, G.R., and Barrioneuvo, G. (2001). Voltage-gated sodium channels shape subthreshold EPSPs in layer 5 pyramidal neurons from rat prefrontal cortex. J. Neurophysiol. *86*, 1671–1684.

Herlitze, S., Garcia, D.E., Mackie, K., Hille, B., Scheuer, T., and Catterall, W.A. (1996). Modulation of Ca^{2+} channels by G protein $\beta\gamma$ subunits. Nature *380*, 258–262.

Hines, M.L., and Carnevale, N.T. (2001). NEURON: a tool for neuroscientists. Neuroscientist *7*, 123–135.

Jiang, Y., Lee, A., Chen, J., Cadene, M., Chait, B.T., and MacKinnon, R. (2002a). Crystal structure and mechanism of a calcium-gated potassium channel. Nature *417*, 515–522.

Jiang, Y., Lee, A., Chen, J., Cadene, M., Chait, B.T., and MacKinnon, R. (2002b). The open pore conformation of potassium channels. Nature *417*, 523–526.

Johnston, D., Hoffman, D.A., Colbert, C.M., and Magee, J.C. (1999). Regulation of back-propagating action potentials in hippocampal neurons. Curr. Opin. Neurobiol. *9*, 288–292.

Jung, H.Y., Mickus, T., and Spruston, N. (1997). Prolonged sodium channel inactivation contributes to dendritic action potential attenuation in hippocampal pyramidal neurons. J. Neurosci. *17*, 6639–6646.

Kontis, K.J., and Goldin, A.L. (1997). Sodium channel inactivation is altered by substitution of voltage sensor positive charges. J. Gen. Physiol. *110*, 403–413.

Lee, A., Wong, S.T., Gallagher, D., Li, B., Storm, D.R., Scheuer, T., and Catterall, W.A. (1999). Calcium/calmodulin binds to and modulates P/Q-type calcium channels. Nature *399*, 155–159.

Li, M., West, J.W., Lai, Y., Scheuer, T., and Catterall, W.A. (1992). Functional modulation of brain sodium channels by cAMP-dependent phosphorylation. Neuron *8*, 1151–1159.

Li, M., West, J.W., Numann, R., Murphy, B.J., Scheuer, T., and Catterall, W.A. (1993). Convergent regulation of Na^+ channels by protein kinase C and cAMP-dependent protein kinase. Science *261*, 1439–1442.

Linford, N.J., Cantrell, A.R., Qu, Y., Scheuer, T., and Catterall, W.A. (1998). Interaction of batrachotoxin with the local anesthetic receptor site in transmembrane segment IVS6 of the voltage-gated sodium channel. Proc. Natl. Acad. Sci. USA *95*, 13947–13952.

Margolskee, R.F., McHendry-Rinde, B., and Horn, R. (1993). Panning transfected cells for electrophysiological studies. Biotechniques *5*, 906–911.

Maurice, N., Mercer, J., Chan, C.S., Hernandez-Lopez, S., Held, J., Tkatch, T., and Surmeier, D.J. (2004). D2 dopamine receptor-mediated modulation of voltage-dependent Na^+ channels reduces autonomous activity in striatal cholinergic interneurons. J. Neurosci. *24*, 10289–10301.

Meisler, M.H., Kearney, J., Ottman, R., and Escayg, A. (2001). Identification of epilepsy genes in human and mouse. Annu. Rev. Genet. *35*, 567–588.

Mickus, T., Jung, H., and Spruston, N. (1999). Properties of slow, cumulative sodium channel inactivation in rat hippocampal CA1 pyramidal neurons. Biophys. J. *76*, 846–860.

Mitrovic, N., George, A.L., Jr., and Horn, R. (2000). Role of domain 4 in sodium channel slow inactivation. J. Gen. Physiol. *115*, 707–718.

Murphy, B.J., Rossie, S., DeJongh, K.S., and Catterall, W.A. (1993). Identification of the sites of selective phosphorylation and dephosphorylation of the rat brain sodium channel alpha subunit by cAMP-dependent protein kinase and phosphoprotein phosphatases. J. Biol. Chem. *268*, 27355–27362.

Nau, C., Wang, S.Y., Strichartz, G.R., and Wang, G.K. (1999). Point mutations at N434 in D1–S6 of μ1 Na^+ channels modulate binding affinity and stereo selectivity of local anesthetic enantiomers. Mol. Pharmacol. *56*, 404–413.

Numann, R., Catterall, W.A., and Scheuer, T. (1991). Functional modulation of brain sodium channels by protein kinase C phosphorylation. Science *254*, 115–118.

Ong, B.H., Tomaselli, G.F., and Balser, J.R. (2000). A structural rearrangement in the sodium channel pore linked to slow inactivation and use dependence. J. Gen. Physiol. *116*, 653–662.

O'Reilly, J.P., Wang, S.Y., and Wang, G.K. (2001). Residue-specific effects on slow inactivation at V787 in D2–S6 of $Na_V1.4$ sodium channels. Biophys. J. *81*, 2100–2111.

Ragsdale, D.S., McPhee, J.C., Scheuer, T., and Catterall, W.A. (1994). Molecular determinants of state-dependent block of Na^+ channels by local anesthetics. Science *265*, 1724–1728.

Rossie, S., and Catterall, W.A. (1987). Cyclic AMP-dependent phosphorylation of voltage-sensitive sodium channels in primary cultures of rat brain neurons. J. Biol. Chem. *262*, 12735–12744.

Rossie, S., and Catterall, W.A. (1989). Phosphorylation of the α subunit of rat brain sodium channels by cAMP-dependent protein kinase at a new site containing Ser^{686} and Ser^{687}. J. Biol. Chem. *264*, 14220–14224.

Rossie, S., Gordon, D., and Catterall, W.A. (1988). Identification of an intracellular domain of the sodium channel having multiple cyclic AMP-dependent phosphorylation sites. J. Biol. Chem. *262*, 17530–17535.

Rudy, B. (1978). Slow inactivation of the sodium conductance in squid giant axons. Pronase resistance. J. Physiol. *283*, 1–21.

Ruff, R.L., and Cannon, S.C. (2000). Defective slow inactivation of sodium channels contributes to familial periodic paralysis. Neurology *13*, 2190–2192.

Schumacher, M.A., Rivard, A.F., Bachinger, H.P., and Adelman, J.P. (2001). Structure of the gating domain of a calcium-activated potassium channel complexed with calcium/calmodulin. Nature *410*, 1120–1124.

Sigel, E., and Baur, R. (1988). Activation of protein kinase C differentially modulates neuronal Na^+, Ca^{2+}, and gamma-aminobutyrate type A channels. Proc. Natl. Acad. Sci. USA *85*, 6192–6196.

Smith, R.D., and Goldin, A.L. (1996). Phosphorylation of brain sodium channels in the I–II linker modulates channel function in *Xenopus* oocytes. J. Neurosci. *16*, 1965–1974.

Smith, R.D., and Goldin, A.L. (1997). Phosphorylation at a single site in the brain sodium channel is necessary and sufficient for current reduction by protein kinase A. J. Neurosci. *17*, 6086–6093.

Struyk, A.F., and Cannon, S.C. (2002). Slow inactivation does not block the aqueous accessibility to the outer pore of voltage-gated Na channels. J. Gen. Physiol. *120*, 509–516.

Stuart, G. (1999). Voltage-activated sodium channels amplify inhibition in neocortical pyramidal neurons. Nat. Neurosci. *2*, 144–150.

Stuart, G., and Haussner, M. (2001). Dendritic coincidence detection of EPSPs and action potentials. Nat. Neurosci. *4*, 63–71.

Surmeier, D.J., and Kitai, S.T. (1997). State-dependent regulation of neuronal excitability by dopamine. Nihon Shinkei Seishin Yakurigaku Zasshi *17*, 105–110.

Surmeier, D.J., Eberwine, J., Wilson, C.J., Cao, Y., Stefani, A., and Kitai, S.T. (1992). Dopamine receptor subtypes colocalize in rat striatonigral neurons. Proc. Natl. Acad. Sci. USA *89*, 10178–10182.

Todt, H., Dudley, S.C., Jr., Kyle, J.W., French, R.J., and Fozzard, H.A. (1999). Ultra-slow inactivation in μ1 Na^+ channels is produced by a structural rearrangement of the outer vestibule. Biophys. J. *76*, 1335–1345.

Vedantham, V., and Cannon, S.C. (1998). Slow inactivation does not affect movement of the fast inactivation gate in voltage-gated Na^+ channels. J. Gen. Physiol. *111*, 83–93.

Vedantham, V., and Cannon, S.C. (2000). Rapid and slow voltage-dependent conformational changes in segment IVS6 of voltage-gated sodium channels. Biophys. J. *78*, 2943–2958.

Vilin, Y.Y., Fujimoto, E., and Ruben, P.C. (2001). A single residue differentiates between human cardiac and skeletal muscle Na^+ channel slow inactivation. Biophys. J. *80*, 2221–2230.

Vilin, Y.Y., Makita, N., George, A.L., Jr., and Ruben, P.C. (1999). Structural determinants of slow inactivation in human cardiac and skeletal muscle sodium channels. Biophys. J. *77*, 1384–1393.

Wang, S.Y., and Wang, G.K. (1997). A mutation in segment IS6 alters slow inactivation of sodium channels. Biophys. J. *72*, 1633–1640.

Wang, D.W., Makita, N., Kitabatake, A., Balser, J.R., and George, A.L., Jr. (2000). Enhanced sodium channel intermediate inactivation in Brugada syndrome. Circ. Res. *87*, 37–43.

West, J.W., Numann, R., Murphy, B.J., Scheuer, T., and Catterall, W.A. (1991). A phosphorylation site in the Na^+ channel required for modulation by protein kinase C. Science *254*, 866–868.

Xiong, W., Li, R.A., Tian, Y., and Tomaselli, G.F. (2003). Molecular motions of the outer ring of charge of the sodium channel: do they couple to slow inactivation? J. Gen. Physiol. *122*, 323–332.

Yarov-Yarovoy, V., Brown, J., Sharp, E.M., Clare, J.J., Scheuer, T., and Catterall, W.A. (2001). Molecular determinants of voltage-dependent gating and binding of pore-blocking drugs in transmembrane segment IIIS6 of the Na channel α subunit. J. Biol. Chem. *276*, 20–27.

Yarov-Yarovoy, V., McPhee, J.C., Idsvoog, D., Pate, C., Scheuer, T., and Catterall, W.A. (2002). Role of amino acid residues in transmembrane segments IS6 and IIS6 of the Na^+ channel α subunit in voltage-dependent gating and drug block. J. Biol. Chem. *277*, 35393–35401.

Zagotta, W.N., Olivier, N.B., Black, K.D., Young, E.C., Olson, R., and Gouaux, E. (2003). Structural basis for modulation and agonist specificity of HCN pacemaker channels. Nature *425*, 200–205.

Zhao, Y., Scheuer, T., and Catterall, W.A. (2004a). Reversed voltage-dependent gating of a bacterial sodium channel with proline substitutions in the S6 transmembrane segment. Proc. Natl. Acad. Sci. USA *101*, 17873–17878.

Zhao, Y., Yarov-Yarovoy, V., Scheuer, T., and Catterall, W.A. (2004b). A gating hinge in sodium channels; a molecular switch for electrical signaling. Neuron *41*, 859–865.